Chemical Science International Journal

Volume 32, Issue 6, Page 90-107, 2023; Article no.CSIJ.110082
ISSN: 2456-706X
(Past name: American Chemical Science Journal, Past ISSN: 2249-0205)

Isolation, Characterisation and Corrosion Inhibition Evaluation of 1, 3, 5-Trimethoxymethylbenzenefrom Seeds Extract of *Cola nitida* on Mild Steel Surface in Hyhrochloric Acid Solution

Mboso I. Obodom [a*], Okon U. Abakedi [a] and Inemesit A. Akpan [a]

[a] Department of Chemistry, University of Uyo, P.M.B.1017, Uyo, Akwa Ibom State, Nigeria.

Authors' contributions

This work was carried out in collaboration among all authors. Author MIO designed the study, performed the weight loss, potetntiodynamic polarization and impedance spectroscopy measurements and wrote the first draft of the manuscript. Author OUA performed quantum chemical studies and managed the analyses of the study. Author IAA wrote the protocol and managed the literature searches. All authors read and approved the final manuscript.

Article Information

DOI: 10.9734/CSJI/2023/v32i6874

Open Peer Review History:
This journal follows the Advanced Open Peer Review policy. Identity of the Reviewers, Editor(s) and additional Reviewers, peer review comments, different versions of the manuscript, comments of the editors, etc are available here: https://www.sdiarticle5.com/review-history/110082

Original Research Article

Received: 03/10/2023
Accepted: 06/12/2023
Published: 11/12/2023

ABSTRACT

Corrosion inhibition of Mild steel in 1 M hydrochloric acid solution by 1, 3, 5-trimethoxymethylbenzene (TMMB) isolated from seeds extract of *Cola nitida* was studied using

**Corresponding author: E-mail: mbosoobodom979@gmail.com;*

weight loss, potentiodynamic polarization and electrochemical impedance spectroscopic methods. TMMB was isolated from seeds of *C. nitida* by 72 hours maceration of the chopped seeds with dichloromethane. Filtered and concentrated extract was subjected to a combination of vacuum liquid, column and thin layer chromatographic techniques. The isolated compound was characterized using Fourier Transform Infra-Red (FT-IR) spectrophotometer, proton nuclear magnetic resonance ($^{+}$H-NMR), C^{13} – NMR and DEPT-135 NMR spectrophotmeters. The results showed that the inhibition efficiency recorded by the weight loss method increased with the increase in TMMB concentration, but decreased with increasing temperature. The inhibition efficiencies recorded by the potentiodynamic polarization and electrochemical impedance spectroscopic methods also increased with increase in the concentration of TMMB. The calculated thermodynamic parameters showed that the corrosion inhibition process was endothermic and spontaneous in nature. Potentiodynamic polarization measurements confirmed that TMMB worked as a mixed – type inhibitor considering the value of E_{corr}being less than 85 mV. Impedance measurement revealed that the charge transfer resistance offered by TMMB to the migration of aggressive ions on the surface of mild steel in acidic solution was enough to impede corrosion. The best line of fit to the adsorption of TMMB onto mild steel surface was found in Temkin isotherm. Formation of protective dense film on the steel surface in the presence of TMMB compared to the blank was revealed by scanning electron microscopy. The molecular structure of TMMB was optimized using Gausian 09 with density functional theory [DFT/B3LYP/6-31G (d,p)]. Physical adsorption has been proposed for the adsorption of TMMB onto mild steel surface.

Keywords: Corrosion; corrosion Inhibitor; cola nitida; mild steel; acidic solution; weight loss; potentiodynamic polarization; electrochemical Impedance spectroscopy; density functional, theory; temkin isotherm.

1. INTRODUCTION

Materials for construction and some components of oil and gas industries made of mild steel rods, sheets and pipes are often exposed to industrial processes involving acidic solutions. This paves the way for industrial processes such as pickling, chemical and electrochemical etching and industrial acid descaling. ‘’The metallic components are susceptible to corrosive actions, which are retrogressive and interfacial reactions of a material (metal, ceramic and polymer) with its environment resulting in consumption of the material’’ [1] and they deteriorate on continued usage.

‘’The use of inhibitors in corrosion prevention and control in aggressive environments is the most cost-effective. Most of the efficient inhibitors are organic compounds that contain heteroatoms such as nitrogen (N), sulphur (S) and oxygen (O) atoms. π-electrons and suitable functional groups in organic compounds also contribute to the corrosion inhibitory properties of these compounds. These atoms are found to have higher basicity and electron density and thus act as inhibitors and are the active centers for corrosion inhibition. The inhibition efficiency conforms to the sequence O <N <S <P” [2]. ‘’The use of corrosion inhibitors that are biodegradable, in addition to being ecologically acceptable, has made plant products good alternatives to synthesized organic compounds” [3]. A number of investigations have been conducted on extracts of different parts of plant materials as potential mild steel corrosion inhibitors in acidic media, thus: cashew waste [4]; *Jatropha tanjorensis* stem bark [5], *Pentaclethramacrophylla Bentham* roots [6]; *Cumimum cyminum* extract [7]; Papaya Leaves [8]; Cassava leaf [9]; water melon wastes [10]; coconut shell [11]; *Gmelina arborea* root extract [12] and *Vernonia amygdalina* extract [13].

Cola belongs to the family of *Sterculiaceae* [14, 15]. The five species of edible cola nuts genus include: *C. nitida*, *C. acuminata*, *C. ballayi*, *C. verticillata* and *C. sphaerocarpa*. The latter three species are not known to be cultivated [15]. *C. nitida* is referenced to have phytochemicals that possess extensive conjugation with substantial π – electron systems and as well contain heteroatoms such as N, S, O or heterocyclic ring in their structures that serve as rally points for interaction with the metal surface [16,1,15,17]. These characteristics enhance the potential of the phytochemicals in the seeds extract of *C. nitida* to inhibit corrosion. Therefore, this research is inclined to investigate the corrosion inhibitory potentials of eco-friendly and less toxic isolated phytochemicals from the seeds of *C. nitida,* as a green corrosion inhibitor.

2. METHODOLOGY

2.1 Plant Material and Extraction Method

Pods having fresh and mature seeds of *C. nitida* were harvested from a plantation in Mbikpong, a rural settlement in Ibesikpo/Asutan Local Government Area of Akwa Ibom State and identified by a taxonomist in the Department of Pharmacognosy and Natural Medicine, Faculty of Pharmacy, University of Uyo, Nigeria with a Voucher No. of UUPH 46. The pods were dissected with a sharp object and the seeds were collected and rinsed with water, cut into pieces, crushed and dried at room temperature (30 ± 2 ^{o}C) for 24 hours. It was then put through comparative extraction in which ethanol, acetone, methanol, ethyl acetate and dichloromethane (DCM) were used to macerate 400 g per solvent (2.5 L) in glass extraction jars for 72 hours and re-macerated for another 72 hours for maximum yield. The filtrates were concentrated using Grant GLS400 water-bath and a preliminary weight loss test was performed on the extracts and DCM extract was affirmed the most active fraction. This was weighed (85 g) and preserved in a refrigerator.

2.2 Purification of DCM Extract

Inherent components in DCM fraction of the extract were subjected to vacuum liquid chromatography (VLC) in order to enhance separation using the following solvent systems: 100 % hexane, 70% hexane: 30% DCM, 50% hexane: 50% DCM (re-macerated), 30% hexane: 70% DCM, 100% DCM, 70% DCM: 30% ethyl acetate, 50% DCM: 50% ethyl acetate, 30% DCM: 70% ethyl acetate and 100% ethyl acetate. Based on the spectra of thin layer chromatographic characteristics, the fractions obtained were pooled, thus:V_1 = 100% hexane + 70% hexane:30% DCM (38.7 g); V_2 = 50% hexane:50% DCM (61.5 g); V_3 = 50% hexane:50% DCM + 30% hexane:70% DCM (85.1 g); V_4 = 100% DCM + 70% DCM: 30% ethyl acetate (50.9 g); and V_5 = 50% DCM: 50% ethyl acetate + 30% DCM: 70% ethyl acetate + 100% ethyl acetate (87.3 g). Initial gravimetric tests on the pooled VLC fractions showed that corrosion inhibition efficiencies were in the following order: V_5 (89%) > V_3 (85 %) > V_1 (83 %) > V_4 (77 %) > V_2 (71%) and this necessitated the choice of V_5 as the sample.

Gradient elution with n-hexane containing increasing quantity of dichloromethane followed by increasing quantities of ethyl acetate and methanol (MeOH) was used on V_5 (87.3 g) loaded onto silica gel column (C1) chromatography (Merck, 60-120 mesh). Eluates of 20 mL were obtained and examined on silica TLC plates (Merck, Germany) in DCM (100%) using p-anisaldehyde-sulphuric acid as spray reagent. Eighty-four (84) eluates were obtained and bulked into eight fractions [A = $O1_{1-12}$(4.9 g), B= $O1_{13-23}$(9.2 g), C = $O1_{24-31}$(8.2 g), D = $O1_{32-59}$(5.8 g), E = $O1_{60-69}$(8.6 g), F = $O1_{70-77}$(16.1 g), G = $O1_{78-81}$ (15.9 g)and H = $O1_{82-84}$(10.2 g)] based on their TLC characteristics; silica gel solvent systems were: 100 % DCM, DCM (2): MeOH (8), DCM (8): MeOH (2) and Ethyl acetate(100%). Based on the TLC characteristics, bulk fraction code named G (114.3 g) was subjected to further purification process by means of normal phase column (C2) chromatography and gradient-eluted with ethyl acetate containing increasing quantities of methanol. 20 mL each of the eluates were collected, monitored on silica TLC plates (Merck, Germany) in DCM (100%) and DCM (8): methanol (2) using p-anisaldehyde-sulphuric acid as spray reagent. Thirty-eight eluates were obtained and bulk into five sub-fractions, thus: A1 = $O2_{1-4}$(2.5 g), B1 = $O2_{5-7}$ (1.3 g), C1 = $O2_{8-15}$(6.8 g), D1 = $O2_{16-35}$(4.1 g) and E1 = $O2_{36-38}$(2.1 g) based on their TLC characteristics. Sub-fraction D1 was colorless from column two (C2) giving single spot on TLC plate with R_F of 0.82, confirmed pure and code named D1.

2.2.1 Characterisation of isolated phytochemical

The isolated compound code named D1 (with single spot on TLC plate) was subjected to Fourier transform infrared (FT-IR) spectrophotometer, proton (^{1}H), carbon-13 (^{13}C) and distortionless enhancement by polarization transfer-135 (DEPT-135) nuclear magnetic resonance (NMR) spectrophotometers.

2.3 Mild Steel Coupons

The mild steel sheet used was procured from John & Sons Nigeria Limited, Uyo, Akwa Ibom State. The steel which had the chemical composition (w/w%): C (0.12), Mn (0.85), S (0.06), P (0.05), Si (0.09) and Fe (98.83). Mechanically, the steel was pressed - cut into coupons of 3.0 cm x 2.0 cm x 0.05 cm. At the center of each coupon, a small hole was drilled to facilitate total immersion in the corrodent using glass rod and hook. These coupons were

abraded with emery papers of different grades (P60X, 220 and 450) to obtain smooth finished surfaces. The coupons were rinsed with deionized water to get rid of organic impurities, washed in ethanol to remove grease and thereafter in acetone to remove oil. The cleaned coupons were preserved over calcium chloride in desiccators prior to use.

The dimension of the coupons for electrochemical experiment was 1.0 cm x 1.0 cm x 0.05 cm. They were also polished to a smooth finish.

2.4 Weight Loss Measurements

Weight loss measurements were performed at total immersion condition of the coupons without stir of the test solutions using glass rod and hook in 100 ml of 1M HCl solution containing different concentrations of D1 (0.1 x 10^{-4} gL^{-1}, 0.5 x 10^{-4} gL^{-1}, 1.0 x 10^{-4} gL^{-1}, 2.0 x 10^{-4} gL^{-1} and 5.0 x 10^{-4} gL^{-1}) and blank, respectively, in a beaker maintained at 303 K. One coupon was placed in each beaker. Mild steel coupons were retrieved from the inhibited and blank solutions at intervals of two hours, immersed in 20% NaOH solution containing 200 gL^{-1} of zinc dust, scrubbed with bristle brush, washed in distilled water, dried in acetone and reweighed [18] to determine weight loss with respect to time. This was done for five consecutive times giving a total of ten hours per temperature. The weight loss was taken to be the difference between the initial weight and the weight of the coupons at a given time for the chosen temperature range. The procedure was repeated at 313 K, 323 K and 333 K. From the data, corrosion rate (CR) measured in $mgcm^{-2}$ h^{-1}, surface coverage (θ) and percentage inhibition efficiency (IE %) were determined using the following equations [19].

$$\mathrm{CR} = \frac{\mathrm{W_1 - W_2}}{\mathrm{St}} \quad (1)$$

where $W_1$is the mass in grams (g) of mild steel coupon before immersion, $W_2$is the mass (g) of mild steel coupon after immersion, S is the total surface area (in cm^{-2}) of the coupon and t is the corrosion time in hours.

$$\theta = \frac{CR_o - CR}{CR_o} \quad (2)$$

$$IE\ \% = \theta\ x\ 100 \quad (3)$$

where CR_o and CR are corrosion rates of the mild steel coupon in 1.0 M HCl in the absence and presence of the extracts, respectively.

2.5 Electrochemical Method

Electrochemical experiments were conducted using the conventional three-electrode cell with a platinum counter electrode (CE) and a saturated calomel electrode (SCE) coupled to a fine lugging capillary as the reference electrode (RE). Ohmic contribution was minimized by placing the lugging capillary closed to the working electrode (WE) which the prepared mild steel coupon was presented in a square form of dimension 1.0 cm x 1.0 cm. The electrode was immersed in the test solution at an open circuit potential (OCP) for thirty minutes to stabilize before measurements could be taken. All electrochemical measurements were taken with the sample immersed in the blank, maximum and minimum concentrations of the test solutions at 303 K using Gamry 600+ Potentiostat/Galvanostat/ZRA Advanced Electrochemical System linked to a computer. The electrochemical set-up was sealed with butyl stoppers where the electrodes and nitrogen pipe providing N_2 gas for deaeration could pass through. Prior to the electrochemical test, the glass cells were sterilized in an autoclave. Both the working electrode and the counter electrodes were further sterilized using 75% ethanol and kept under ultraviolet rays prior to the experiment.

2.4.1 Potentiodynamic polarization measurements

"The polarization curve was recorded under potentiodynamic polarization at the condition of air atmosphere and controlled by a personal computer. After the open circuit potential had been established, potentiodynamic polarization curves were obtained at a scan rate of 1 mVS^{-1} in the potential range from -0.25 V to 0.25 V. Application of a small potential drop (ΔE) generates a corresponding current flow (Δl)" [20].

The corrosion rate of the system was determined using corrosion current density, i_{corr}. The linear portions of the anodic and cathodic Tafel curves were extrapolated to the corrosion potential (E_{corr}) and the corrosion current (i_{corr}) axes. All potentials were measured against SCE. The surface coverage (θ) and the percentage inhibition efficiency (% IE), were evaluated by the application of Equations (4) and (5) [21], thus:

$$\theta = \frac{i^o_{corr} - i_{corr}}{i^o_{corr}} \quad (4)$$

$$IE\% = \theta\ x\ 100 \quad (5)$$

The values of corrosion current density in the absence and presence of inhibitor are given by $i_{corr}^{o}$and i_{corr} (μA cm^{-2}), respectively [22, 23].

2.4.2 Electrochemical impedance spectroscopic measurements

The measurements of electrochemical impedance spectroscopy were carried out over a frequency range of 10 Hz to 100,000 Hz at 303 K using amplitude of 5 mV RMS peak-to-peak with an alternating current signal at the open circuit potential and at air atmosphere. The impedance data were recorded using Nyquist plots and the charge transfer resistance,R_{ct}, was obtained from the diameter of the semicircle in the plot. The percentage inhibition efficiency (% IE) was calculated from R_{ct}values obtained from the impedance measurements according to the models bellows, thus:

$$\theta = \frac{R_{ct} - R_{ct}^{o}}{R_{ct}} \quad (6)$$

$$IE\% = \theta \; x \; 100 \quad (7)$$

charge transfer resistances in the presence and absence of the inhibitor are given by R_{ct}(Ωcm^{-2}) and R_{ct}^{o}(Ωcm^{-2}), respectively [24,25].

2.5 Scanning Electron Microscopy (SEM)

Samples were ground with SiC paper having 1000 grit, washed in distilled water and then in ethanol, dried in compressed air and placed in a fume hood. Morphological survey was conducted on 1 cm x 1 cm area of the surface of mild steel coupons before and after immersion in both blank and solution with inhibitors. Thermo Fisher Scientific Prisma E scanning electron microscopy was used. Measurements were taken at a magnification of 300 μ.

2.6 Quantum Chemical Studies

Corrosion inhibition mechanism of D1 on mild steel in hydrochloric solution was studied using Gaussian 09 and density functional theory (DFT) with the basis set of B3LYP/6 – 31G (d,p) in the aqueous phase. Possible physical properties of D1 that make it effective as corrosion inhibition were evaluated using theoretical study.

3 RESULTS AND DISCUSSION

3.1 Characterisation of D1

D1 was obtained in a substantial quantity (4.1 g) as a colorless crystalline solid soluble in dimethyl sulphur (ll) oxide (DMSO) solvent. Spectroscopic results on D1 revealed, thus: FT- IR (KBr, cm^{-1}): 3153, 3116, 3015 (C-H aromatic), 2829 (C-H aliphatic), 1655 (C=C), 1454 (CH_3 deformation), 1223 (C-O stretching) (Fig. 1).

^{1}H NMR (60 MHz, DMSO-d_6): δ7.95 (s, 3H, Ar-H), 3.85 (s, 6H, 3 x CH_2OCH_3), 1.24 (s, 9H, 3 x CH_2OCH_3) ppm (Fig. 2).

C-13 NMR (15 MHz, DMSO-d_6): No information was deduced from the spectra due to absence of visible compound peaks.

DEPT-135 (15 MHz, DMSO-d_6): No information was deduced from the spectra due to absence of visible compound peaks.

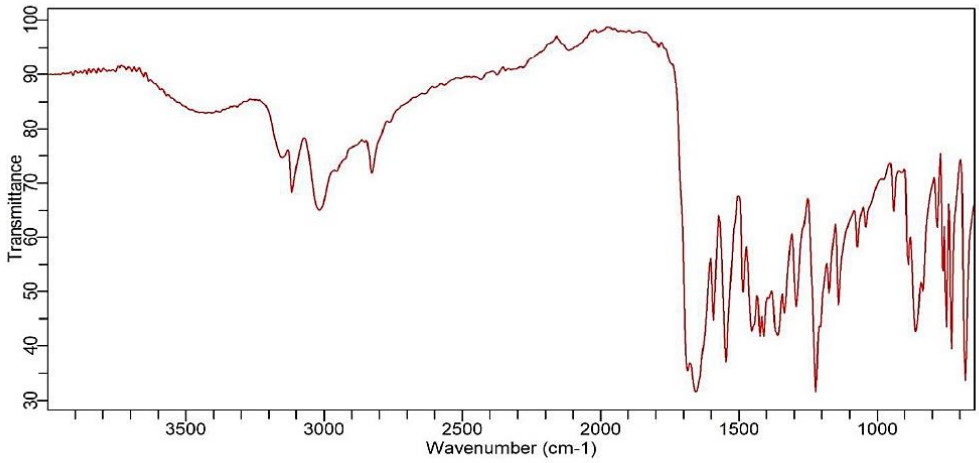

Fig. 1. Fourier Transform – Infrared (FT- IR) Spectra for D1

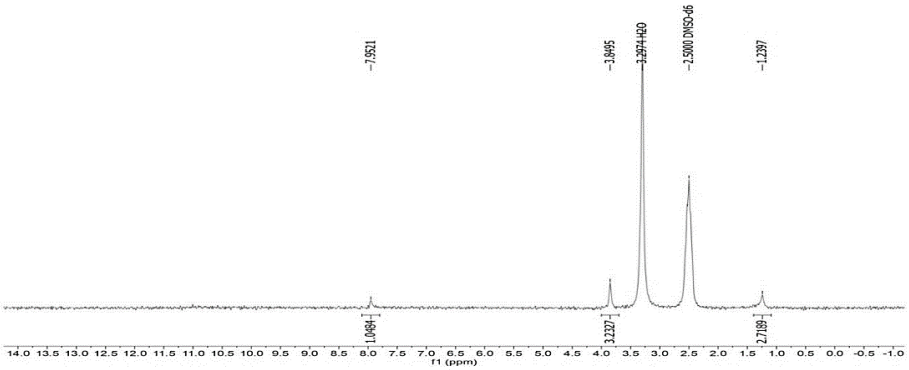

Fig. 2. Proton nuclear magnetic (^{1}H NMR) spectra for D1.

Based on the available pieces of information from FT – IR and ^{1}H NMR spectra, the following structure was elucidated, thus:

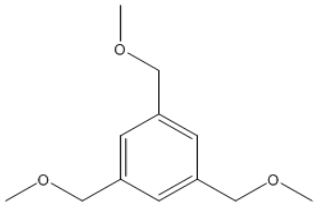

Fig. 3. 1, 3, 5-Trimethoxymethylbenzene (TMMB)

Therefore, D1 was elucidated and identified as 1, 3, 5-trimethoxymethylbenzene abbreviated TMMB

3.2 Weight Loss Results

3.2.1 Effect of TMMB Concentration on Inhibition Efficiency

Variation of inhibition efficiency with respect to the concentration of TMMB in 1 M HCl solution is presented in Fig. 4. It is observed that the inhibition efficiency increased with increase in TMMB concentration. The highest inhibition efficiency obtained at 303 K was 55.83% at 5.0 x 10^{-4} g L^{-1} (Table 1). "This implies that there is an interaction between TMMB molecules and the steel surface. The data indicate that there is a higher degree of surface coverage of mild steel surface with increase in the concentration of TMMB, thereby impeding the actions of aggressive ions and of course, inhibiting corrosion" [26].

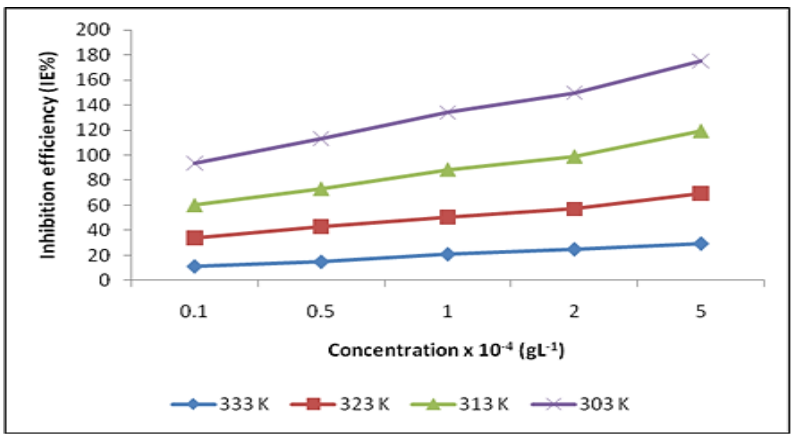

Fig. 4. Effect of 1, 3, 5-trimethoxymethylbenzene (TMMB) on the corrosion inhibition efficiency of mild steel at different temperatures

Table 1: Calculated values of weight loss, corrosion rate and inhibition efficiency formild steel corrosion in 1 M HCl in the absence and presence of different concentrations of TMMB

Inhibitor Conc. (x 10^{-4})	Weight loss (g)				Corrosion rate (mg cm^{-2} hr^{-1})				Inhibition efficiency (%)			
	303 K	313 K	323 K	333 K	303 K	313 K	323 K	333 K	303 K	313 K	323 K	333 K
Blank	0.150	0.248	0.317	0.421	2.40	3.97	5.07	6.74	-	-	-	-
0.1 g L^{-1}	0.100	0.184	0.214	0.361	1.60	2.94	3.92	5.94	33.33	25.94	22.68	11.42
0.5 g L^{-1}	0.090	0.174	0.198	0.358	1.44	2.78	3.64	5.73	40.00	29.97	28.21	14.99
1.0 g L^{-1}	0.082	0.154	0.184	0.333	1.31	2.46	3.57	5.33	45.42	38.04	29.59	20.92
2.0 g L^{-1}	0.074	0.144	0.156	0.317	1.18	2.30	3.44	5.01	50.83	42.07	32.15	24.78
5.0 g L^{-1}	0.066	0.124	0.132	0.238	1.06	1.98	3.04	4.77	55.83	50.13	50.13	29.23

3.2.2 Effect of temperature on inhibition efficiencY

Table 1 displays a pattern of corrosion rate (CR) considering a total immersion time of 10 hours in the absence and presence of TMMB at different temperatures. It is seen that CR increases with increase in temperature and decreases with increase in the concentration as it varies, thus: 1.06 mg cm^{-2} hr^{-1} at 303K, 1.98 mg cm^{-2} hr^{-1} at 313 K, 3.04 mg cm^{-2} hr^{-1} at 323 K and 4.77 mg cm^{-2} hr^{-1} at 333 K considering 5.0 x 10^{-4} g L^{-1} of TMMB (Table 1). At higher temperatures, effective adsorption of TMMB molecules onto the surface of mild steel reduces. Therefore, corrosion rates rise at higher temperatures [27]. Besides, weight loss trend is seen to decrease as the concentration of TMMB increases. This is linked to the protection of mild steel as the degree of surface coverage (θ) increased in proportion to the concentration of TMMB. The weight losses by TMMB at 303 K were 0.100 g and 0.066 g at 0.1 x 10^{-4} g L^{-1} and 5.0 x 10^{-4} g L^{-1}, respectively (Table1). [28] reported a similar trend.

Corrosion rate, CR, evaluated from the weight loss measurements in acidic medium is related to temperature by the Arrhenius like equation:

$$log\ \mathrm{CR} = \log \mathrm{A} - \frac{\mathrm{E_a}}{2.303\mathrm{RT}} \quad (8)$$

where E_a ($Jmol^{-1}$) is the energy of activation, A (mg cm^{-2} h^{-1}) is the pre-exponential constant of Arrhenius, R ($Jmol^{-1}$ K^{-1}) is the universal gas constant and T (K) is the absolute temperature. Energies of activation were evaluated from the slopes of the plot of $\log CR$ versus $\frac{1}{T}$ (Fig. 5) and presented in Table 2. "It is obvious that the E_a values in the presence of TMMB are higher than the E_a of the blank. These values reveal that the presence of TMMB raised the energy of activation of the metal dissolution reaction. The higher values of energy of activation in the presence of TMMB compared to the blank and the decrease in the percentage inhibition efficiency with increase in temperature are pointers to physical adsorption process" [29]. Therefore, the mechanism of adsorption of TMMB on mild steel surface is by physical adsorption.

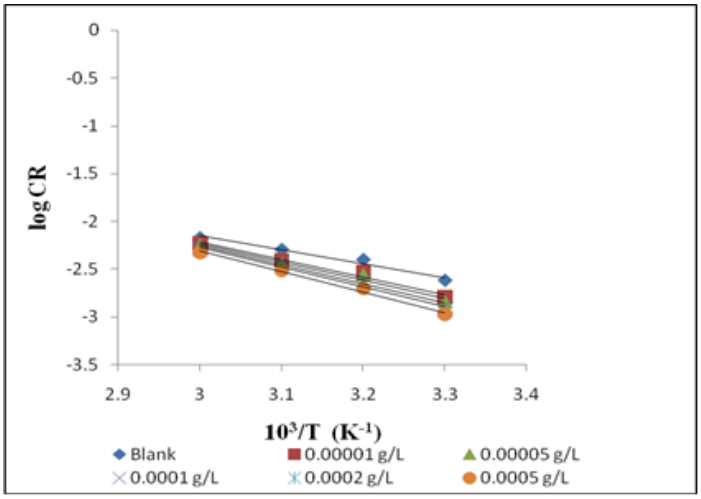

Fig. 5. Arrhenius plot of log CR versus 1/T for mild steel coupons in 1 M HCl solution in the absence and presence of different concentrations of TMMB

Table 2. Thermodynamic parameters for mild steel corrosion in 1 M HCl solution in the absence and presence of different concentrations of TMMB at 303 – 333 K

Inhibitor	Concn.M x 10^{-4}	E_a(kJ mol^{-1})	ΔH^o_{ads} (kJ mol^{-1})	- ΔS^o_{ads}(J $K^{-1}mol^{-1}$)
	Blank	27.95	25.16	211.63
TMMB	0.1	35.04	32.45	190.94
	0.5	36.76	34.06	186.44
	1.0	38.10	35.46	182.68
	2.0	39.63	36.80	179.03
	5.0	40.78	38.47	174.66

The values of enthalpy change, ΔH^o_{ads}, and entropy change of adsorptions, ΔS^o_{ads}, were determined from the transition state equation [30] as stated in equation (9), thus:

$$CR = \frac{RT}{Nh}\exp\left(\frac{\Delta S^o_{ads}}{R}\right)\exp\left(-\frac{\Delta H^o_{ads}}{RT}\right) \quad (9)$$

where N (mol^{-1}) is the Avogadro's number, h (Js) is the Planck's constant, R (J K^{-1} mol^{-1}) is the universal gas constant and T is the absolute temperature. Equation (9) is rearranged as follows:

$$ln\left(\frac{CR}{T}\right) = \left[ln\left(\frac{R}{Nh}\right) + \frac{\Delta S^o_{ads}}{R}\right] - \frac{\Delta H^o_{ads}}{RT} \quad (10)$$

Linear plot of $log(\frac{CR}{T})$ versus $\frac{1}{T}$ (Fig. 6) with slope and intercept of $-\frac{\Delta H^o_{ads}}{R}$ and $\left[ln\left(\frac{R}{Nh}\right) + \frac{\Delta S^o_{ads}}{R}\right]$, respectively, were obtained. The slopes were used to determine the enthalpy change of adsorption (ΔH^o_{ads}) and intercepts were used to obtain the entropy change of adsorption (ΔS^o_{ads}) as presented in Table 3.The positive values of ΔH^o_{ads} connote that the adsorption process of TMMB on to the surface of mild steel is accompanied heat adsorption and it is endothermic in nature. The negative values of ΔS^o_{ads} imply that the adsorption process is linked to a decrease in entropy and this is paramount to the adsorption of TMMB onto the surface of mild steel surface [31, 32]. Similar trend of result had been reported by [26].

3.2.3 Adsorption consideration

It is imperative to evaluate an experimental best fit adsorption isotherm to the surface coverage data in order to assess the interactions between the molecules of TMMB and the mild steel surface. The adsorption of TMMB onto mild steel surface was tested with Temkin, Langmuir and El-Awady adsorption isotherms. The best fit was obtained with Temkin isotherm given as equation (11) [33, 34, 35].

$$e^{f\theta} = K_{ads}C \quad (11)$$

where θ is the surface coverage, K_{ads} (L mol^{-1}) is the equilibrium constant of adsorption process, C (g L^{-1}) is the inhibitor concentration and f is the factor of energetic inhomogeneity describing the molecular interactions in the adsorption layer (f = -2a) [36].

K_{ads} is related to the standard free energy of adsorption, ΔG^o_{ads}, through the equation (8) [37].

$$log\ K_{ads} = 1.744 - \frac{\Delta G^o_{ads}}{2.303RT} \quad (12)$$

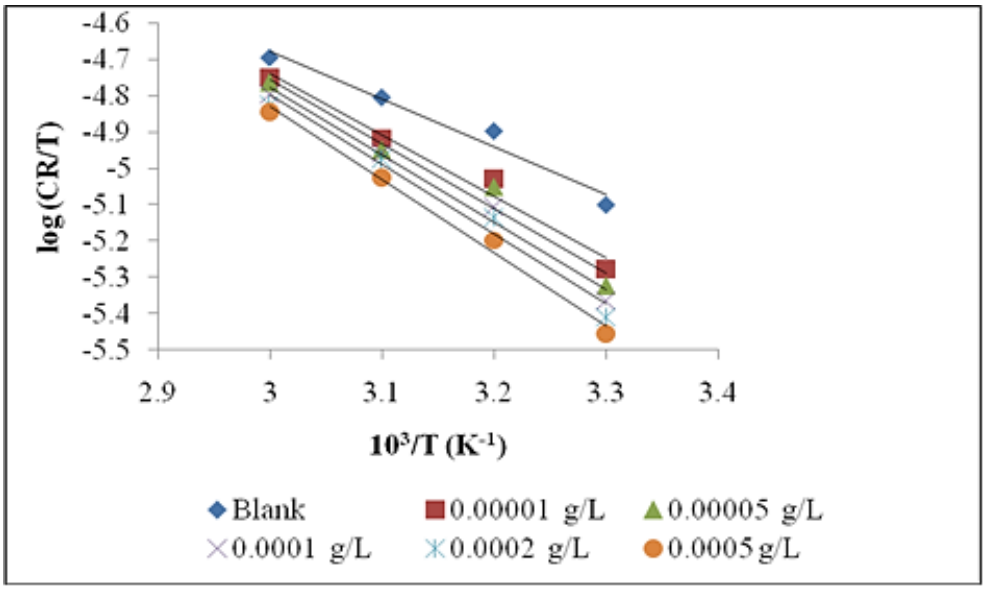

Fig. 6. Transition State plot for mild steel coupons in 1M HCl in the absence and presence of different concentrations of TMMB.

A linear plot of surface coverage (θ) versus logarithm of inhibitor concentration (*log C*) with correlation coefficients (R^2) within the range $0.930 \leq R^2 \leq 0.996$ obtained for TMMB (Fig. 7) indicates that TMMB adsorption best fits to Temkin isotherm. The values of K_{ads} signify the strength of adsorption between adsorbate and adsorbent. Large values of K_{ads} reflect efficient adsorption and hence better inhibition efficiency [38]. The values of K_{ads} from Table 3 are very low and this implies weak interaction (physical adsorption) between the molecules of TMMB and the mild steel surface. The negative values of 'a' connote existence of attraction in the adsorption layer [39].

The negative values of Gibss' free energy change of adsorption, ΔG^o_{ads}, (Table 3) implies that the adsorption of TMMB onto the surface of mild steel was a spontaneous process.

3.3 Potentiodynamic Polarization Measurements

"The presence of TMMB in the test solutions pushed the cathodic and anodic locations to the minimum current magnitudes. This means that corrosion at these locations was retarded by TMMB. Polarization parameters such as corrosion current densities (i_{corr}), corrosion potential (E_{corr}), cathodic Tafel slope (β_c) and anodic Tafel slope (β_a) were generated from the Tafel plot (Fig. 8) and used in the calculation of percentage inhibition efficiency (IE%) as presented in Table 4 at different concentrations of TMMB. The values of β_c and β_a were largely affected by the inclusion of TMMB in the blank. When the shift in E_{corr} is higher than 85 mV, the inhibitor can be grouped as either anodic or cathodic, but if the shift is lower than 85 mV, the inhibitor is categorized mixed-type" [40]. The E_{corr} values as presented in Table 4 are far less than the threshold value of 85 mV. This confirms that TMMB is a mixed-type corrosion inhibitor with the inhibition of both cathodic and anodic reactions. Similar results had been reported by [41]. Percentage inhibition efficiencies of 67% and 48% were recorded at 5.0 x10^{-4} g L^{-1} and 0.1 x10^{-4} g L^{-1} concentrations of TMMB, respectively. This means that i_{corr} reduces considerably with respect to increase in the concentration of TMMB in the blank (Table 4). Therefore, percentage inhibition efficiency improves upon increase in the concentration of the inhibitor [42].

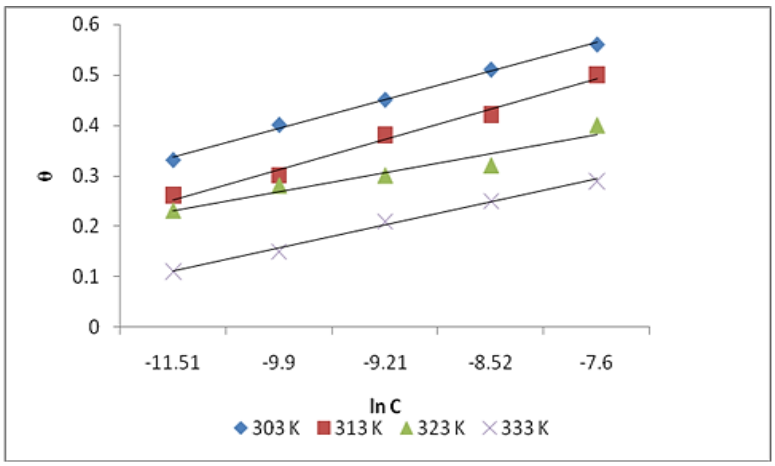

Fig. 7. Temkin adsorption isotherm for mild steel corrosion in 1 M HCl solution in the absence and presence of different concentrations of TMMB

Table 3. Some adsorption parameters from Temkin isotherm for mild steel coupons in 1 MHCl containing different concentrations of TMMB at 303 – 333 K

Inhibitor	Temp (K)	Intercept	Slope	K(L mol^{-1})	f	- a	-ΔG(kJ/mol)	R^2
TMMB	303	0.279	0.057	133.44	17.54	8.77	22.45	0.996
	313	0.192	0.060	24.55	16.67	8.33	18.78	0.986
	323	0.192	0.038	156.56	26.32	13.16	24.36	0.930
	333	0.064	0.046	4.02	21.74	10.87	14.97	0.994

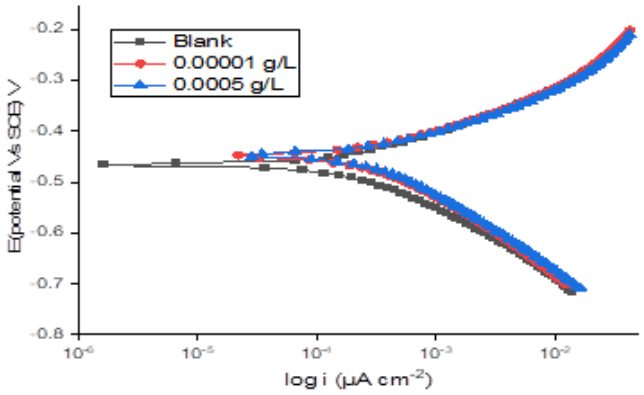

Fig. 8. Polarization curve of mild steel in 1.0 HCl solution in the absenceand presence of different concentrations of TMMB at 303 K

Table 4. Potentiodynamic polarization parameters from Tafel plots for mild steel immersed in 1.0 M HCl solution in the absence and presence of different concentrations of TMMB at 303 K

Inhibitor	Concn.(g/L)	-E_{corr}(mV vs SCE)	i_{corr}(μA/cm^2)	β_c (mV dec^{-1})	β_a (mV dec^{-1})	IE%
	Blank	453.11	365.01	154	65	-
TMMB	0.1x10^{-4}	458.66	190.05	140	98	48
	5.0 x10^{-4}	461.54	118.65	124	86	67

3.4 Electrochemical IMPEDANCE Spectroscopy

A one-time constant phase element (CPE) circuit (Fig. 9) was used to analyze the electrochemical impedance data generated from a sample area of 1.0 cm^2 at chi squared error of 6.081 x 10^{-6}, relative standard error ranging from 0.084 to 0.788 and the measurement errors in impedance data ≤ 0.2466. This was achieved using the ZSimpwin software application.

"Impedance measurements were performed to evaluate the characteristics and kinetics of the metal/solution interface and how the corrosion reactions are obstructed by the inhibitor" [43].

"A plot of Z''_{Im} versus Z'_{Re} (Nyquist) of mild steel immersed in the absence and presence of TMMB is presented in Fig. 10. It is observed that impedance of the mild steel increases with increase in the concentration of TMMB. The plot shows one incomplete capacitive loop corresponding to the charge transfer reaction which is dependent on either electron transfer at the metal surface or on the electron conduction through the surface film" [44]. It is observed that the change in concentration of TMMB had no effect on the shape of the impedance behavior and this suggests that TMMB exhibits similar corrosion inhibition mechanism on mild steel at various concentrations.

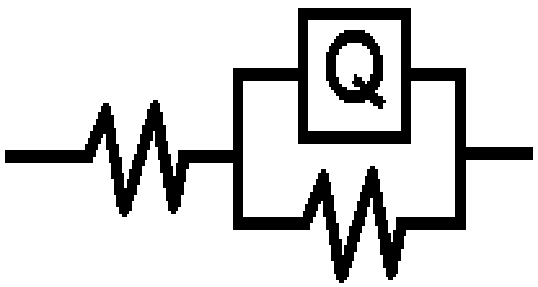

Fig. 9. One time constant phase element (CPE) circuit

The impedance plots (Fig. 10) are not perfect semicircles due to frequency dispersion caused by coarseness and surface fractions of the metal [45]. The impedance of the CPE is obtained according to equation (13) [46,47], thus:

$$Z_{CPE} = Y_o^{-1}(jw)^{-n} \quad (13)$$

where Y_o(1.182 x 10^{-3} at 5.0 x10^{-4} gL^{-1} and 1.250 x 10^{-3} at 0.1 x10^{-4} gL^{-1} of TMMB) and n (0.817 ≤ n ≤ 0.830) are associated with CPE (Table 6). "j^2 = –1 regarded as the imaginary axis, ω stands for angular frequency in $rads^{-1}$, W denotes the impedance factor and n is the considered shifting factor which explains the surface heterogeneity, impurities and surface fractions of the metal" [41].

"Chloride ions from the electrolyte (acid used) adsorb onto the metal surface and the presence of TMMB in test solution gradually displaces the chloride ions and their presence at relatively low inhibitor concentration may induce adsorption. More so, chloride ions play a role in the adsorption of protonated inhibitor molecules by specially adsorbing to the metal surface, thus creating a negative charge towards the solution" [48]

Introduction of TMMB in the acid solution promoted the radius of the imperfect loop which reflects corrosion inhibition and corresponds to the charge transfer resistance, R_{ct}, of the mild steel surface. Diameter of the depressed incomplete semicircles at high frequency is often regarded as the charge transfer resistance, R_{ct}. The percentage inhibition efficiency, *IE%*, of TMMB for the mild steel electrode is evaluated using equation (14), thus:

$$IE\ \% = \frac{R_{ct} - R_{ct}^{o}}{R_{ct}}\ x\ 100 \quad (14)$$

where charge transfer resistances in the presence and absence of TMMB are given by R_{ct}(Ω cm^{-2}) and R_{ct}^{o} (Ω cm^{-2}), respectively [26]. The value of R_{ct} increases in direct proportion to the concentration of TMMB, with percentage inhibition efficiency of 58% at 5.0 x10^{-4} gL^{-1} at 303 K (Table 6).

Bode plot of phase angle against logarithm of frequency (*log f)* in the absence and presence of TMMB is presented in Fig. 11 and phase angle peaks at different frequencies of the corrosion media at 303 K are obvious. Asymmetric overlap of peaks for each concentration of TMMB is observed at 35.1 Hz as 64.5° for 5.0 x 10^{-4} gL^{-1}, at 29.12 Hz as 58.1° for 0.1 x 10^{-4} gL^{-1} and at 37.99 Hz as 51.8° for the blank (Fig. 11), respectively. This implies that TMMB inhibits mild steel corrosion in acidic media as the phase angle of the inhibitor solution is greater than that of the blank.

Table 5. Some Electrochemical Impedance Parameters of Mild Steel in 1M HCl Solutions in the absence and presence of TMMB at 303 K

TMMB Concn.	R_S	R_{ct}	Q		IE %
	($\Omega.cm^{-2}$)	($\Omega.cm^{-2}$)	Y_o x 10^{-3} (S s^n cm^{-2})	n	
Blank	2.914	76.550	0.831	0.856	-
0.1 x 10^{-4} g L^{-1}	2.947	125.490	1.250	0.817	40
5.0 x 10^{-4} g L^{-1}	2.851	182.260	1.182	0.830	58

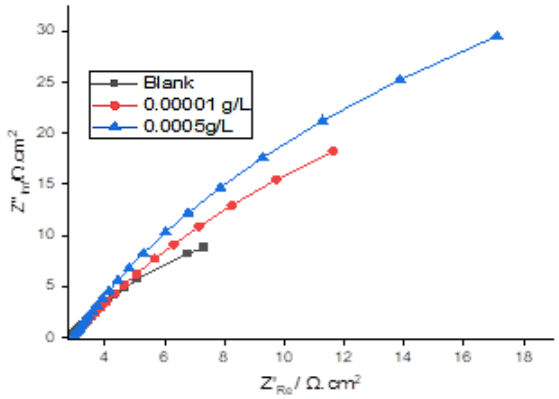

Fig. 10. Nyquist plot of mild steel in 1.0 HCl solution in the absence and presence of different concentrations of TMMB at 303 K

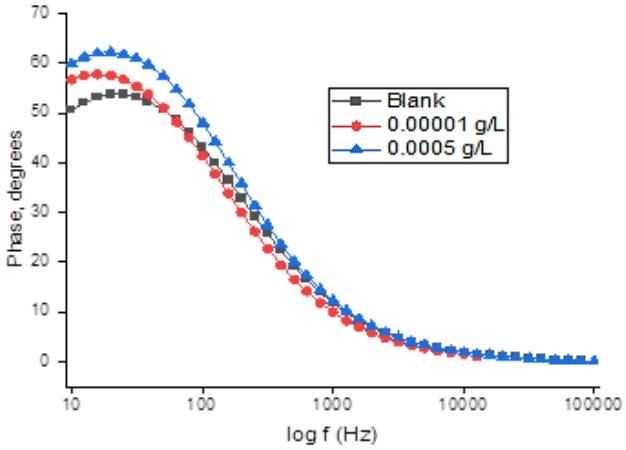

Fig. 11. Bode Plot of mild steel in 1.0 M HCl solution in the absence and presence of different concentrations of TMMB at 303 K

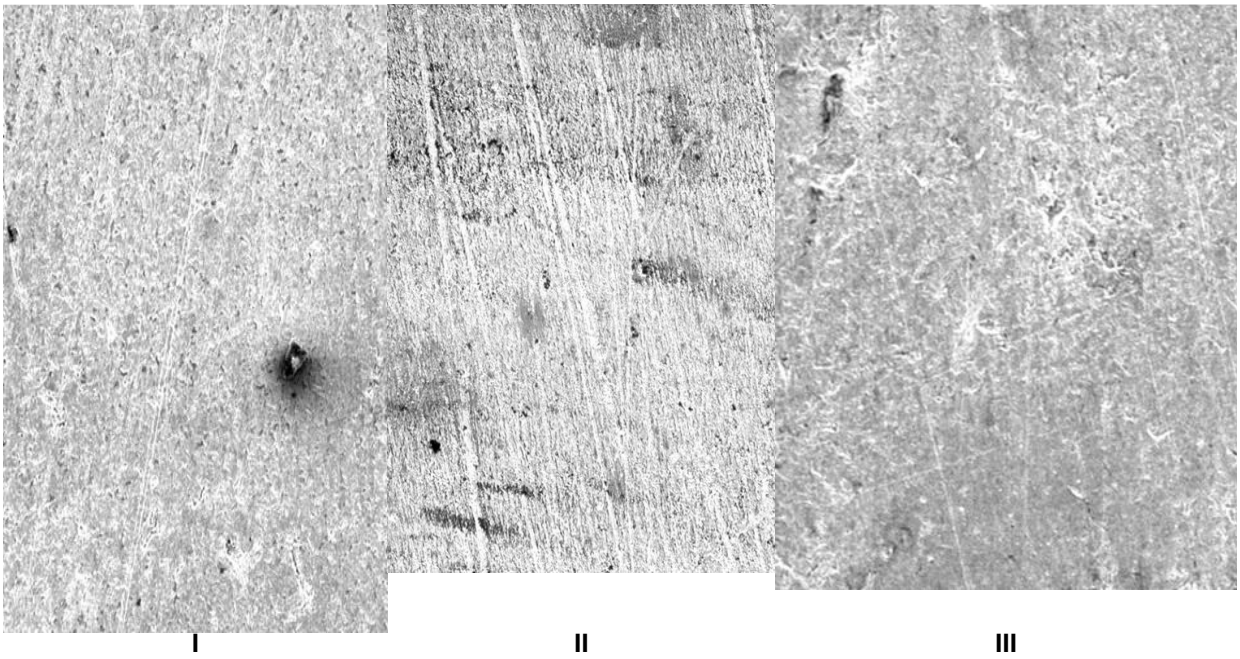

Fig. 12. SEM image of mild steel surface exposed to (I) 1.0 M HCl solution (blank), (II) 1.0 M HCl containing 0.1 x 10^{-4} gL^{-1} of TMMB, and (III)1.0 M HCl containing 5.0 x 10^{-4} gL^{-1} of TMMB

3.5 Scanning Electron Microscopy (SEM)

Micrographs of the mild steel coupons placed in 1 M hydrochloric acid solution in the absence and presence of 1, 3, 5-Trimethoxymethylbenzene (TMMB)were taken at a magnification of 300 µm and are presented in Fig. 12 (I – III). Fig. 12 (I) exposes localized pitting of the coupon in blank. The aggressive nature of Cl^- and H^+ ions in the interfacial dissolution layer of the steel is responsible for the rough morphology of mild steel in the blank [43]. Similar trends of results were obtained by other workers [26]. The mild steel coupons in the presence of TMMB at 0.1 x10^{-4} gL^{-1} (Fig. 12 II) and at 5.0 x10^{-4} gL^{-1} (Fig. 12 III) are smoother than that of the blank. The differences in textural properties of the micrographs arise from the formation of dense film at the metal-solution interface by TMMB, hence a reduction in the substrate(mild steel) deterioration rate. Consequently, TMMB at 5.0 x10^{-4} gL^{-1} provided a better protection to the mild steel than TMMB at 0.1 x10^{-4} gL^{-1} as seen in the micrographs (Fig. 12: I – III).

3.6 Quantum Chemical Studies

Optimized structure of 1, 3, 5-trimethoxymethylbenzene (TMMB), lowest unoccupied molecular orbital, E_{LUMO} and highest occupied molecular orbital, E_{HOMO} are presented in Fig. 13 (I - III). Quantum chemical assessment reveals that frontier molecular orbital energies, E_{HOMO} and E_{LUMO}, are necessary parameters to determine the reactivity of chemical species by theoretical technique [44]. Quantum chemical parameters were calculated using equations (15 - 19) and are presented in Table 6. Information on the ability of a molecule to donate electrons to appropriate acceptor molecule with empty molecular orbital is obtained from E_{HOMO} and it is -6.570 eV with TMMB. The inhibition efficiency of an inhibitor is linked to the value of E_{HOMO} such that high value of E_{HOMO} reflects on high inhibition efficiency [49]. The energy gap, ΔE_{gap}, determines the reactivity of molecules. Inhibitors with low ΔE_{gap} should have good inhibition efficiencies because the energy required to remove the valence electron in a molecule is low and TMMB with ΔE_{gap} (6.248 eV) is an average corrosion inhibitor. The number of electrons transferred (ΔN) reveals that TMMB (ΔN = 0.220). In view of the positive values of ΔN, it implies that electrons will be donated to the metal surface by TMMB. It is important to note that in as much as the value of ΔN is less than 3.6, the inhibition efficiency increases with the ability of the molecules to donate electrons to the metal surface [50]. The electronegativity, χ, of TMMB is 3.446 eV is lower than the work function of Fe(110) surface given as 4.82 eV and this points to the fact that electrons migrate from the inhibitor to the Fe surface. Since the value of χ for TMMB is lower, movement of electrons from TMMB to the Fe surface is to be expected.

Global hardness, η, and global softness, σ, are used to define how an atom resists the deformation of its electron cloud and they are 3.124 eV and 0.320 eV^{-1}, respectively, implying that TMMB is a hard molecule. Therefore, TMMB is an average inhibitor from quantum studies.

Energy gap, $\Delta E = E_{LUMO} - E_{HOMO}$ (15)

Electronegativity, $\chi = -\frac{1}{2}(E_{HOMO} - E_{LUMO})$ (16)

Global hardness, $\eta = -\frac{1}{2}(E_{LUMO} - E_{HOMO})$ (17)

Global softness, $\sigma = -\frac{1}{\eta}$ (18)

Number of transported electrons between metal surface and the inhibitor,

$$\Delta N = \frac{(\phi - \chi_i)}{2\eta_i} \quad (19)$$

Where ϕ (4.82 eV) is the work function of iron [Fe(110)], a modeled surface configuration of iron used for the evaluation.

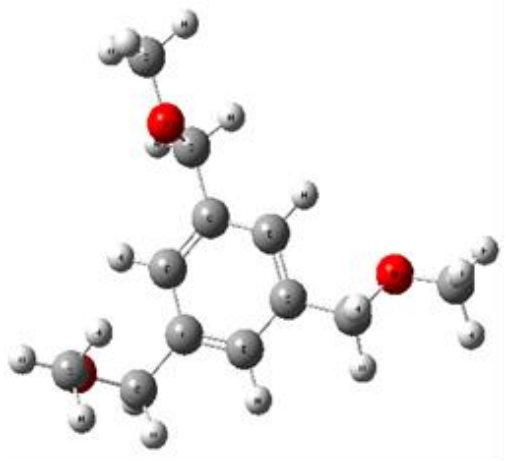

(I)

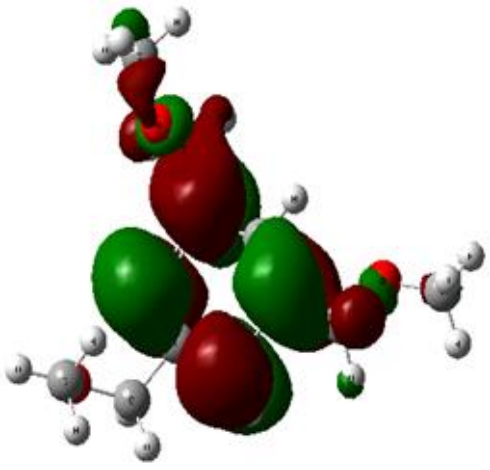

(II)

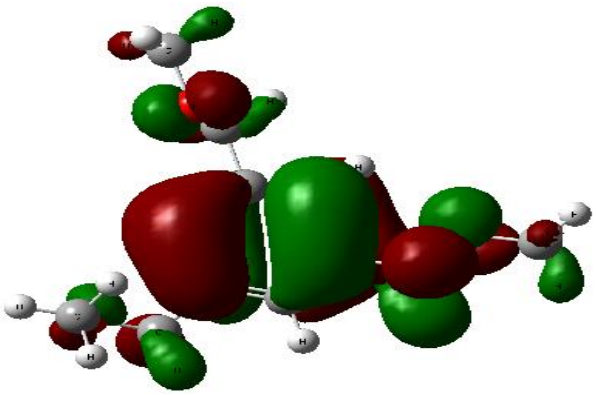

(III)

Fig. 13. Structure of 1, 3, 5-Trimethoxymethylbenzene (TMMB): (I) optimized, (II) LUMO and (III) HOMO

Table 6. Quantum chemical parameters for TMMB at geometry optimization

Inhibitor	E_{HOMO} (eV)	E_{LUMO} (eV)	ΔE_{gap}(eV)	IE(eV)	EA(eV)	χ(eV)	η(eV)	σ(eV^{-1})	ΔN
TMMB	-6.570	-0.322	6.248	6.570	0.322	3.446	3.124	0.320	0.220

4. CONCLUSION

The study reveals that 1, 3, 5 – trimethoxymethylbenzene (TMMB), a phytochemical isolated from fresh and mature seeds of *Cola nitida* inhibited the corrosion of mild steel in 1 M HCl solution. Inhibition efficiency of TMMB was found to increase with increase in concentration, but decreased with increase in temperature. Adsorption of TMMB onto the mild steel surface fitted to Temkin isotherm. The negative values of ΔG^{o}_{ads} are indicative of the spontaneity of the corrosion inhibition process and the endothermic nature of TMMB adsorption process is confirmed by the positive values of ΔH^{o}_{ads} . The negative values of ΔS^{o}_{ads} indicate less disorder of TMMB molecules on the mild steel surface and hence a stronger adsorption of TMMB molecules on mild steel surface. TMMB is a mixed-type inhibitor based on its E_{corr} value. The inhibition efficiency obtained from weight loss, potentiodynamic polarization, electrochemical impedance spectroscopy and quantum chemical studies were in agreement. Dense film formed was seen in the micrographs of the steel and it was responsible for retarding the migration of aggressive ions in the corrodent and thereby inhibiting mild steel corrosion in hydrochloric acid solution. And from the quantum chemical studies, the electronegativity of TMMB (3.446 eV) is lower than the function work function of Fe (4.82 eV). This implies that electrons will migrate from the inhibitor to the surface of mild steel. With these results, TMMB is concluded to be a corrosion inhibitor of steel in hydrochloric acid solution.

ACKNOWLEDGEMENTS

Tertiary Education Trust (TETFund) in Nigeria provided financial support for the study and it is greatly acknowledged. The ingenuity and interest in the line of the study was pivoted by Savior Umoren and Emmanuel Essien. Paul Thomas and Desire Christopher assisted in the maceration, vacuum liquid and column chromatographic techniques, steps taken to isolate and purify the phytochemical. The effort of Iniobong Sam in facilitating the polishing process of the coupons cannot be ignored. Inime Udoh assisted so well in the electrochemical and scanning electron microscopic techniques. All the contributions made by these people to the success of this study are appreciated and acknowledged.

COMPETING INTERESTS

Authors have declared that no competing interests exist.

REFERENCES

1 Jyothi S, Subba Rao YV, Samuel Ratnakumar PS.Natural Product as Corrosion Inhibitors in Various Corrosive

Media: A Review.Raysayan J. Chem. 2019;12(2):537–544.

2 Hadisaputra S, Purwoko AA, Hakim A, Prasetyo N, Hamdiani S. Corrosion Inhibition Properties of Phenyl Phthalimide Derivatives against Carbon Steel in the AcidicMedium: DFT, MP2, and Monte Carlo Simulation Studies. ACS Omega.2022;7(37):33054-33066.

3 Perez N. Electrochemistry and Corrosion Science, 2nd Edition, London, Springer. 2016;243–59.

4 Olawale O**,** Bello JO, Akinbami P. A Study on Corrosion Inhibitor of Mild Steel in Hydrochloric Acid using Cashew Waste.International Journal of Modern Engineering Research. 2015;5(8):25-30.

5 Abakedi OU, Sunday MV, James MA. Mild Steel Corrosion Inhibition in Acidic Medium by *Jatropha tanjorensis* Stem Bark Extract. International Journal of Chemical Studies. 2021;9(3):9-13.

6 Lebe N, Georoge N, Justus N, Nneka E, Peter E. Aqueous Extracts of Roots of *Pentaclethra macrophylla,* Bentham, as eco-friendly Corrosion Inhibition for Mild Steel in 0.5 M KOH Medium. International Journal of Materials and Chemistry. 2016;6(1):12-18.

7 Sribharathy S, Rajendran S. *Cuminum cyminum* Extracts as Eco-friendly Corrosion Inhibitor for Mild Steel in Seawater. Research Article. 2013;1-7.

8 Kavitha N, Manjula P, Anandha Kumar N. (2014). Syneristic Effect of Papaya Leaves Extract –Zn^{2+}in Corrosion Inhibition of Mild Steel in Aqueous Medium. Research Journal of ChemicalScience. 2014;4(8):88-93.

9 Diah RG, Emriadi AA, Mai E. Water Extracts of Cassava Leaf as Corrosion Inhibitor for Mild Steel in Sulfuric Acid Solution. Journal of Chemical and Pharmaceutical Research.2015;7(12): 398-405.

10 Odewunmi NA, Umorem SA, Gasem ZM. Watermelon Waste Products as Green Corrosion Inhibitors for Mild Steel in HCl Solution. Journal of EnvironmentalChemicalEngineering. 2015;3(1):286-296.

11 Daramola OO, Adediran AA, Fadumiye AT. Evaluation of the Mechanical Properties and Corrosion Behaviour of Coconut Shell Ash Reinforced Aluminium (6063)Alloy Composites. Leornado Electronic Journal and Practices Technologies. 2015;27:107-119.

12 Abakedi OU, Akpan IA, Ekemini NE. (2018). Inhibition of mild steel corrosion by *Gmelina arborea* root extract in 1 M H_2SO_4 solution. Journal of Materials Science Research and Reviews. 2018;1(1):1–9.

13 Olawale O, Adediran AA, Talabi SI, Nwokocha GC, Ameh AO. Inhibitory Action of *Vernonia amygdalina* Extract (VAE) on the Corrosion of Carbon Steel in Acidic Medium. J. Electrochem. Sci. Eng. 2017;7(3):145-152.

14 The International Plant Names Index (IPNI). Biodiversity Heritage Library, data base;2020.

15 Kanoma AI, Muhammad I, Abdullahi S, Shehu K, Maishanu HM, Isah AD. Qualitative and Quantitative Phytochemical Screening of Cola Nuts (*Cola Nitida and Cola Acuminata*). Journal of Biology, Agriculture and Healthcare. 2014;4(5):2224-3208.

16 Ashmawy AS, Mostafa MA, Abo-Bakr Kamal, Ali GAM, El-Gaby MSA. Corrosion Inhibition of Mild Steel in 1 M HCl by Pyrazolone-sulfonamide Hybrids: Synthesis, Characterization, and Evaluation. Sci Rep.2023;13,18555.

17 Huong DQ, Huong NTL, Nguyet TT, Duong T, Tuan D, Thong NM, Nam PC. Pivotal Role of Heteroatoms in Improving the Corrosion Ability of Thiourea Derivatives. *ACS Omega*. 2020;42: 27655-27666.

18 Sanni O,Iwarere SA, Daramola MO. Introduction: Corrosion Basics and Corrosion Testing in: Electrochemical and Analytical Techniques for Sustainable Corrosion Monitoring. 2023;1-23.

19 Obot IB, Obi-Egbedi NO. Fluconazole as an Inhibitor for Aluminium Corrosion 0.1 M HCl. Colloid Surface: Physio-chemistry. Engineering Aspects. 2008;330:207-212.

20 Nabuk OE, Ebenso EE, Ibok UJ. Adsorption, Synergistic Inhibitive Effect and Quantum Chemical Studies of Ampicillin (AMP) and Halides for the Corrosion of Mild Steel in H_2SO_4. Journal of Applied Electrochemistry. 2010;40:445-456.

21 Roy P, Sukul D. Protein-surfactant Aggregate as Potential Corrosion Inhibitor for Mild Steel in Sulphuric Acid: zein-SDS system. Royal Society of Chemistry Advances. 2015; 5: 1359-1365.

22 Rodriguez JA, Borbolla JC, Arizpe P, Gutierrez E. Mathematical Models

Generated for the Prediction of Corrosion Inhibition Using Different Theoretical Chemistry Simulations. Materials. 2020;13(24):5656

23 Garai S, Garai, S, Jaiasankai P, Singh JK,Elango A. A Comprehensive Study on Crude Methanolic Extract of *Artemisia pallens* (Asteraceace) and its Actives Component as Effective Corrosion Inhibitors of Mild Steel in Acid Solution. Corrosion Science. 2012;60:193-204.

24 De Motte R, Basilico E, Minggant R, Kittel J, Ropital F, Combrade P, Necib S, Deydier V, Crusset D, Marcelin S. A study by electrochemical impedance spectroscopy and surface analysis of corrosion product layers formed during CO_2corrosion of low alloy steel. Corrosion Science. 2020;172:108666.

25 Da Rocha JC, Gomes JAC, D'Elia E. Aqueous extracts of mango and orange peel as green inhibitors for carbon steel in hydrochloric acid solution. Materials Research. 2014;7(6):1590–1605.

26 Obodom MI, Akpan IA, Abakedi OU. Gravimetric and Electrochemical Assessments of the Corrosion Inhibition Potential of *Cola nitida* Seeds Extract on Mild Steel Surface in Hydrochloric Acid (HCl) Solution. Asian Journal of Chemical Sciences.2023;13(6):118 - 131.

27 Abakedi OU, Asuquo JE. Mild Steel Corrosion Inhibition by *Eremomastax polysperma* Leaf Extract in Acidic Medium. Asian Journal of Chemical Sciences. 2016;1(1):1-9.

28 Benchadli A, Attar T, Messaoudi B, Choukchou-Braham E. Polyvinyl Pyrrolidone as a Corrosion Inhibitor for Carbon Steel in a Perchloric Acid Solution: Effect of StructuralSize. HungarianJournal of Industry and Chemistry. 2021;49(1):59–69.

29 Undiandeye JA, Chior TJ, Mohammed A, Offurum JC. Kinetics of the Corrosion of Mild Steel in Petroleum-Water Mixture Using Ethyl Ester of Lard as Inhibitor. AU J.T. 2014;17(3):129-136.

30 Umoren SA. Polypropylene glycol: A novel corrosion inhibitor for ×60 pipeline steel in 15% HCl solution. Journal of Molecular Liquids. 2016;219: 946 – 958.

31 Karhikaiselvi R, Subhashini S. Study of adsorption properties and inhibition of mild steel corrosion in ydrochloric acid media by water soluble composite poly (vinyl alcohol-omethoxy aniline. Journal of the Association of Arab Universities for Basics and Apllied Sciences. 2014;16:74 – 82.

32 Oyekunle DT,Agboola O, Ayeni AO. Corrosion Inhibitors as Building Evidence for Mild Steel: A Review. Journal of Physics: Conference Series. 2019; 1378(3):1742–1758

33 Masel R. Principles of Adsorption and Reaction on Solid Surfaces.nWiley InterScience: Hoboken, New Jersey; 1996.

34 Arshad N, Altaf F, Akram M, Ullah M. Furan and Phenyl Substituted TriazolothiadiazineDerivatives as Copper Corrosion Inhibitors: Electrochemical and DFT Studies. Protection of Metals and Physical Chemistry of Surfaces. 2019; 55(4):770–780.

35 Medupin RO, Ukoba KO, Yoro KO, Tien-Chien Jen. Sustainable approach for corrosion control in mild steel using plant-based inhibitors: a review. Materials Today Sustainability. 2023;22:100373.

36 Kaghazchi L. Nader R, Ramezanzadeh B. Synergistic mild steel corrosion mitigation in sodium chloride containing solution utilizing various mixtures of phytic molecules and Zn^{2+}ions Journal of Molecular Liquids. 2021;323:114589.

37 Kokalj A. Considering the concept of synergism in corrosion inhibition. Corrosion Science. 2021; 212:110922

38 Palumbo G, Berent K, Proniewicz E,Banas J. Guar Gum as an Eco-Friendly Corrosion Inhibitor for Pure Aluminium in 1-M HCl Solution. Materials (Basel). 2019;12(16):2620.

39 Sahakitpichan P, Mahidol C, Disadee W, Ruchirawat S, Kanchanapoom T. Unusual glycosides of pyrrole alkaloid and 4'-hydroxyphenyl ethanamide from leaves of *Moringa oliefera*. Phytochem.2011;72:791–795.

40 Dehghani A, Bahlakeh G, Ramezanzadeh B, Ramezanzadeh M. Detailed Macro-/micro-scale Exploration of the Excellent Active Corrosion Inhibition of a Novel Environmentally Friendly Green Inhibitor for Carbon Steel in Acidic Environment. J. Taiwan Inst. Chem. Eng. 2019;100: 239–261.

41 Lowmunkhong P, Ungthararak D, Sulthivaiyakit P. Tryptamine as a Corrosion Inhibitor of Mild Steel in Hydrochloric Acid Solution. Corrosion Science. 2010;52:30-36.

42 Anadebe VC, Nnaji PC, Okafor NA, Ezeugo JO, Abeng FE, Onukwuli OD. Evaluation of Bitter Kola Leaf Extract as an Anticorrosion Additive for Mild Steel in 1.2 M H_2SO_4 Electrolyte. S. Afr. J. Chem. 2021;75:6–17.

43 Khaled KF, Al-Qahtani MM. The Inhibitive Effect of some Tetrazole Derivatives towards Al Corrosion in Acid Solution: Chemical, Electrochemical and Theoretical Studies. Materials Chemistry and Physics. 2009;113:150-158.

44 Karthick S, Muralidharan S, Lee HS, Kwon SJ, Saraswathy V. Reliability and Long-term Evaluation of GO-MnO_2 Nano Material as a Newer Corrosion Monitoring Sensor for Reinforced Concrete Structures. Cem. Concr. Compos. 2019;100:74–84.

45 Hao X, Dong J, Etim IN, Wei J, Ke W. Sustained Effect of remaining Cementite on the Corrosion Behavior of Ferrite-Pearlite Steel under the Simulated bottom Plate Environment of Cargo Oil Tank. Corros. Sci. 2016;110:296–304.

46 Hao X, Dong J, Wei J, Etim IN, Ke W. Effect of Cu on Corrosion Behavior of Low Alloy Steel under the Simulated bottom Plate Environment of Cargo Oil Tank. Corros. Sci. 2017;121:84– 93.

47 Ikpi ME, Udoh II, Okafor PC, Ekpe UJ, Ebenso EE. Corrosion Inhibition and Adsorption Behaviour of Extracts from Piper guinensis on Mild Steel Corrosion in Acid Media. International Journal of Electrochemical Science.2012;7:12193 – 12206.

48 Al-Bataineh N, Al-Qudah AA, Abu-Orabi S, Bataineh T, Hamaideh RS, Al-Momani IF, Hijazi AK. Use of *Capparis decdua* Extract as a Green Inhibitor for Pure Aluminium Corrosion in Acidic Media. Corrosion Science and Technology. 2022;21(1):9-20.

49 Rajendran M, Keerthika K, Kowsalya M, Devapinam D. Theoretical Studies on Corrosion Inhibition Efficiency of Pyridine Carbonyl Derivatives using DFT Method. Der. Pharma Chem. 2016;8(3):71 – 79.

50 Tan L, Li J, Zeng X. Revealing the Correlation between Molecular Structure and Corrosion Inhibition Characteristics of N-Heterocycles in Terms of Substituent Groups. Materials. 2023;16(6):2148.

Peer-review history:
The peer review history for this paper can be accessed here:
https://www.sdiarticle5.com/review-history/110082